Research Article | Vol. 8, No. 9 | 1 Sep 2017 | BIOMEDICAL OPTICS EXPRESS 4122
Biomedical Optics EXPRESS

Evaluation of collimated polarized light imaging for real-time intraoperative selective nerve identification in the human hand

K. W. T. K CHIN,[1] A. F. ENGELSMAN,[1] P. T. K. CHIN,[2] S. L. MEIJER,[3] S. D. STRACKEE,[4] R. J. OOSTRA,[5] AND T. M. VAN GULIK[1,*]

[1]*Department of Surgery, Academic Medical Center, Meibergdreef 9, 1105 AZ Amsterdam, the Netherlands*
[2]*Condensed Matter and Interfaces, Debye Institute for Nanomaterials Science, Utrecht University, Princetonplein 5, 3584 CC Utrecht, the Netherlands*
[3]*Department of Pathology, Academic Medical Center, Meibergdreef 9, 1105 AZ Amsterdam, the Netherlands*
[4]*Department of Plastic and Reconstructive Surgery, Academic Medical Center, Meibergdreef 9, 1105 AZ Amsterdam, the Netherlands*
[5]*Department of Anatomy, Embryology and Physiology, Academic Medical Center, Meibergdreef 9, 1105 AZ Amsterdam, the Netherlands*
[*]*t.m.vangulik@amc.uva.nl*

Abstract: Intraoperative peripheral nerve lesions are common complications due to misidentification and limitations of surgical nerve identification. This study validates a real-time non-invasive intraoperative method of nerve identification. Long working distance collimated polarized light imaging (CPLi) was used to identify peripheral radial nerve branches in a human cadaver hand by their nerve specific anisotropic optical reflection. Seven *ex situ* and six *in situ* samples were examined for nerves, resulting after histological validation, in a 100% positive correct score (CPLi) versus 77% (surgeon). Nerves were visible during a clinical *in vivo* observation using CPLi. Therefore CPLi is a promising technique for intraoperative nerve identification.

OCIS codes: (170.0170) Medical optics and biotechnology; (170.3880) Medical and biological imaging; (260.1440) Birefringence; (260.5430) Polarization

References and links

1. T. Kretschmer, G. Antoniadis, V. Braun, S. A. Rath, and H. P. Richter, "Evaluation of iatrogenic lesions in 722 surgically treated cases of peripheral nerve trauma," J. Neurosurg. **94**(6), 905–912 (2001).
2. G. Antoniadis, T. Kretschmer, M. T. Pedro, R. W. König, C. P. Heinen, and H. P. Richter, "Iatrogenic nerve injuries: prevalence, diagnosis and treatment," Dtsch. Arztebl. Int. **111**(16), 273–279 (2014).
3. D. McGeorge, M. Sturzenegger, and U. Buchler, "Tibial nerve mistakenly used as a tendon graft. Reports of three cases," J. Bone Joint Surg. Br. **74**(3), 365–366 (1992).
4. R. Y. Chandawarkar, A. L. Cervino, and G. A. Pennington, "Management of iatrogenic injury to the spinal accessory nerve," Plast. Reconstr. Surg. **111**(2), 611–619 (2003).
5. T. G. Weiser, A. B. Haynes, G. Molina, S. R. Lipsitz, M. M. Esquivel, T. Uribe-Leitz, R. Fu, T. Azad, T. E. Chao, W. R. Berry, and A. A. Gawande, "Size and distribution of the global volume of surgery in 2012," Bull. World Health Organ. **94**(3), 201–209 (2016).
6. C. L. Wu and S. N. Raja, "Treatment of acute postoperative pain," Lancet **377**(9784), 2215–2225 (2011).
7. A. Zyluk and P. Janowski, "Results of the treatment of major, complex hand injuries," Pol. Przegl. Chir. **83**(2), 87–94 (2011).
8. S. O. Rogers, Jr., A. A. Gawande, M. Kwaan, A. L. Puopolo, C. Yoon, T. A. Brennan, and D. M. Studdert, "Analysis of surgical errors in closed malpractice claims at 4 liability insurers," Surgery **140**(1), 25–33 (2006).
9. S. P. Johnson, J. M. Adkinson, and K. C. Chung, "Addressing medical errors in hand surgery," J. Hand Surg. Am. **39**(9), 1877–1882 (2014).
10. A. M. Ilyas, M. Ast, A. A. Schaffer, and J. Thoder, "De quervain tenosynovitis of the wrist," J. Am. Acad. Orthop. Surg. **15**(12), 757–764 (2007).
11. A. Deniwar, E. Kandil, and G. Randolph, "Electrophysiological neural monitoring of the laryngeal nerves in thyroid surgery: review of the current literature," Gland Surg. **4**(5), 368–375 (2015).

#286405 https://doi.org/10.1364/BOE.8.004122
Journal © 2017 Received 3 May 2017; revised 18 Jul 2017; accepted 18 Jul 2017; published 16 Aug 2017

Biomedical Optics EXPRESS

12. A. Grayev, S. Reeder, and A. Hanna, "Use of chemical shift encoded magnetic resonance imaging (CSE-MRI) for high resolution fat-suppressed imaging of the brachial and lumbosacral plexuses," Eur. J. Radiol. **85**(6), 1199–1207 (2016).
13. A. Manoliu, M. Ho, D. Nanz, M. Piccirelli, E. Dappa, M. Klarhöfer, F. Del Grande, and F. P. Kuhn, "Diffusion Tensor Imaging of Lumbar Nerve Roots: Comparison Between Fast Readout-Segmented and Selective-Excitation Acquisitions," Invest. Radiol. **51**(8), 499–504 (2016).
14. A. J. Robson, M. S. See, and H. Ellis, "Applied anatomy of the superficial branch of the radial nerve," Clin. Anat. **21**(1), 38–45 (2008).
15. D. Poggio, G. Claret, A. M. López, C. Medrano, E. Tornero, and J. Asunción, "Correlation Between Visual Inspection and Ultrasonography to Identify the Distal Branches of the Superficial Peroneal Nerve: A Cadaveric Study," J. Foot Ankle Surg. **55**(3), 492–495 (2016).
16. F. C. Lee, H. Singh, L. N. Nazarian, and J. K. Ratliff, "High-resolution ultrasonography in the diagnosis and intraoperative management of peripheral nerve lesions," J. Neurosurg. **114**(1), 206–211 (2011).
17. R. W. Koenig, T. E. Schmidt, C. P. Heinen, C. R. Wirtz, T. Kretschmer, G. Antoniadis, and M. T. Pedro, "Intraoperative high-resolution ultrasound: a new technique in the management of peripheral nerve disorders," J. Neurosurg. **114**(2), 514–521 (2011).
18. T. Hussain, L. T. Nguyen, M. Whitney, J. Hasselmann, and Q. T. Nguyen, "Improved facial nerve identification during parotidectomy with fluorescently labeled peptide," Laryngoscope **126**(12), 2711–2717 (2016).
19. S. A. Boppart, "Optical coherence tomography: technology and applications for neuroimaging," Psychophysiology **40**(4), 529–541 (2003).
20. I. Ducic, L. A. Seiboth, and M. L. Iorio, "Chronic postoperative breast pain: danger zones for nerve injuries," Plast. Reconstr. Surg. **127**(1), 41–46 (2011).
21. N. Kosaka, M. Ogawa, P. L. Choyke, and H. Kobayashi, "Clinical implications of near-infrared fluorescence imaging in cancer," Future Oncol. **5**(9), 1501–1511 (2009).
22. M. Finke, S. Kantelhardt, A. Schlaefer, R. Bruder, E. Lankenau, A. Giese, and A. Schweikard, "Automatic scanning of large tissue areas in neurosurgery using optical coherence tomography," Int. J. Med. Robot. **8**(3), 327–336 (2012).
23. K. W. T. K. Chin, A. Meijerink, and P. T. K. Chin, "Interventional nerve visualization via the intrinsic anisotropic optical properties of the nerves," Proc. SPIE **9540**, 95400O (2015).
24. R. Oldenbourg, E. D. Salmon, and P. T. Tran, "Birefringence of single and bundled microtubules," Biophys. J. **74**(1), 645–654 (1998).
25. H. T. Meryman, "Mechanics of freezing in living cells and tissues," Science **124**(3221), 515–521 (1956).
26. Z. Zhu, L. Qiao, Y. Zhao, and S. Zhang, "Optimal freezing and thawing for the survival of peripheral nerves in severed rabbit limbs," Int. J. Clin. Exp. Pathol. **7**(11), 7801–7805 (2014).
27. L. J. Menz, "Structural changes and impairment of function associated with freezing and thawing in muscle, nerve, and leucocytes," Cryobiology **8**(1), 1–13 (1971).
28. K. Tohyama, C. Ide, and T. Osawa, "Nerve regeneration through the cryoinjured allogeneic nerve graft in the rabbit," Acta Neuropathol. **80**(2), 138–144 (1990).

Introduction

Perioperative peripheral nerve injuries are a known and commonly encountered complication of surgical interventions [1]. Even when an intervention seems successful at first glance, this could be complicated by unexpected neural injury. One of the main reasons of accidental nerve injuries during a surgical intervention is the difficulty in distinguishing different tissue types, such as connective tissue and nerves [2, 3]. In particular, small cutaneous sensory branches of peripheral nerves are difficult to identify intraoperatively [4]. Kretschmer et al. showed that the percentage of iatrogenic nerve injuries reaches 17% of the total amount of nerve injuries reported. Their report indicates a substantial number of patients with iatrogenic nerve injury considering the millions of operations that are performed worldwide [5].

In the hand and wrist area dense networks of sensory and motor nerves are present, which increases the risk of perioperative peripheral nerve injuries. The function of these small nerves is paramount in regard to the function of the hand. Transection of these branches leads to significant morbidity in patients due to loss of sensory function [6, 7]. Rogers Jr. et al. showed that visceral or somatic nerve injuries represent approximately 25% of all iatrogenic lesions [8]. In orthopedic surgery, this accounted for 15% of the total medical liability claims in the United States [9]. Therefore, improving intraoperative nerve visualization would greatly help to reduce intraoperative accidental nerve injuries.

Currently, surgeons rely on their anatomical knowledge, blunt dissection techniques and intraoperative neuromonitoring (IONM) combined with preoperative visualization such as MRI, diffusion tensor imaging and ultrasonography to identify nerves [10–14]. Recent

Biomedical Optics EXPRESS

developments in intraoperative nerve visualization can be found in new uses of ultrasonography, fluorescent markers and optical coherence tomography (OCT) [15–19]. However, these methods have their drawbacks; blunt dissection of nerves is not without risk, due to the risk of traction-stretch neuropathy [10, 20]. The use of fluorescent markers is challenging due to potential toxicity, biological side effects and 'low' specificity [21]. As a result of its technical nature, OCT is a non-real-time scanning technique which is best suitable for relatively small areas [22]. Despite these developments, a real-time non-invasive and specific technique for nerve identification is still not available.

Recently, we showed a first proof-of-concept of a new optical concept to visualize the nerves during surgery [23]. Under conventional illumination only minimal visual distinction can be made between different tissue types. As such, collimated polarized light imaging (CPLi) was used as a technique to observe the distinct collimated polarized reflection of the nerve tissue in an animal model [23]. Nerve tissue comprises a strong anisotropic structure in which the microtubules are oriented along the length direction of the axon which induces a distinct rotated linear polarized optical reflection under light [23, 24].This nerve specific polarized optical reflection can be clearly distinguished from the isotropic and anisotropic scattering events typically observed in the surrounding tissue types. The use of polarized and collimated illumination enabled a maximal signal intensity of the nerves, which is vital to maintain a long working distance needed for a real-time surgical intervention. The aim of this study is to adapt and validate the CPLi technique to a system that allows non-invasive nerve visualization in a real-time intraoperative setting in human tissue.

Material and methods

Imaging system and operation

A 'standard' stereo microscope (Olympus SZ3060 series clone) was modified according to the working principle disclosed in our previous publication (Fig. 1) [23]. Figure 1 shows an image of the CPLi modified microscope, which comprises a polarization unit with a rotatable disk consisting of an adhesive linear sheet polarizer (P200A, wavelength: 380 ~700 nm obtained from 3Dlens.com) on the outer rim of the transparent polarizer disk and a separate rotatable inner linear imaging polarizer (B + W). The two LED light sources (3W Cree, UltraFire) contain an adjustable collimation lens. As described in our previous work, the optimal identification of nerve tissue is performed under dynamic rotation of the optical polarizers with respect to the nerve tissue orientation. Therefore, the polarization unit is continuously rotated upon nerve identification, while keeping both polarizers in perpendicular position in respect to each other. Image acquisition was performed from a distance of ± 20 centimeters from the region of interest (ROI) using a scientific camera (ToupCam LCMOS03100KPA) adapted for imaging through the microscope's ocular.

Biomedical Optics EXPRESS

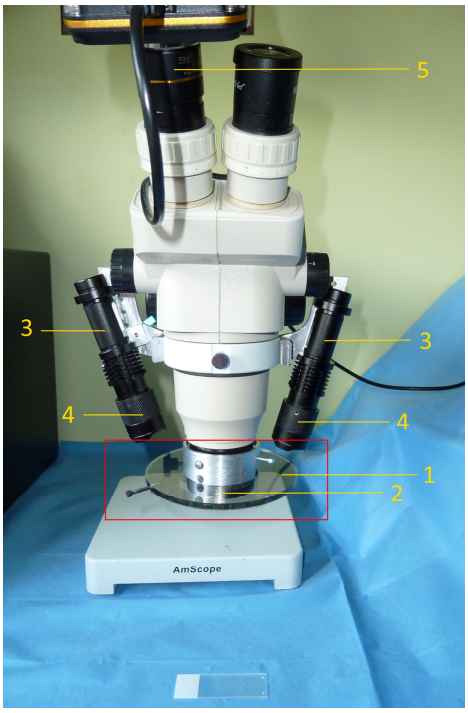

Fig. 1. The stereo microscope with the polarization unit attached underneath (red box). (1) The outer rim of the polarizer disk with a linear polarizer that is aligned perpendicular to the inner linear polarizer (2). 3W Cree LEDs are mounted on each side (3) both equipped with an adjustable collimation lens (4). On top the microscope camera (5) is mounted on the site of the left ocular.

Cadaver tissue

The tissue used for this experiment was a defrosted, fresh frozen human cadaver arm, obtained through the body donation program of the department of Anatomy, Embryology and Physiology at the Academic Medical Center, Amsterdam. The region of interest (ROI) in this study was the dorsoradial part of the hand, more specifically around the superficial branches of the radial nerve around the anatomical snuff box (tabatière region, Fig. 2).

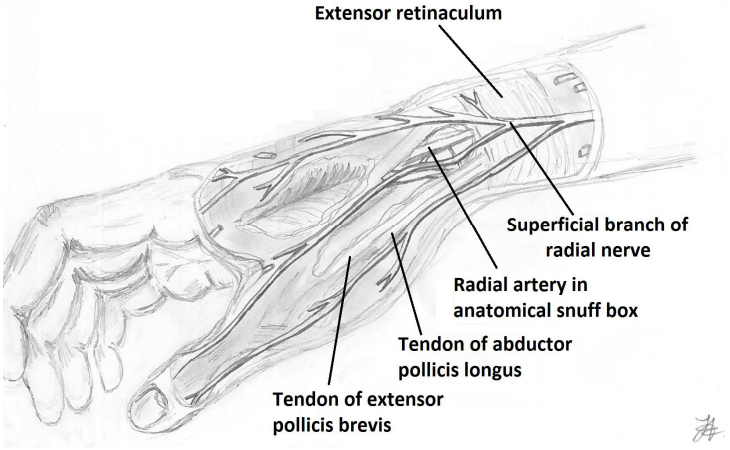

Fig. 2. Illustration of the tabatière region in the human hand.

Biomedical Optics EXPRESS

Effect of freezing on nerves

Potential negative tissue alteration effects on the optical properties due to freezing and defrosting, in particular for nerve tissue was examined using fresh pig tissue (Sus scrofa) obtained from a specialist butcher. Nerves at the joint (wrist) area of the leg were observed using CPLi (Appendix 1).

Visualization and acquisition of cadaver tissue

The observations during the experiment were performed by two persons; the surgeon who exposed the tissue using conventional illumination and an operator who assessed the optical characteristics of the tissues by means of the CPLi. The CPLi operator had ample previous experience with image recognition in chicken tissue using CPLi.

An incision in the skin over tabatière was used to expose the subcutaneous tissue for imaging. Different parts of the superficial subcutaneous ROI were imaged under conventional surgical illumination, followed by image acquisition using the CPLi system, to make a comparison between normal visualization by eye and CPLi of the exposed, superficially located nerve tissue (Fig. 3).

Subsequently, the area underneath the extensor retinaculum around the tendinous sheath of the abductor pollicis longus and extensor pollicis brevis muscles and the tendinous sheath of the extensores carpi radialis were further exposed, to study the deeper-lying anatomical structures in greater detail. The area around the wrist joint (articulatio radiocarpea) was also exposed for larger structures, i.e. the radial artery, larger branches of the radial nerve and the tendons passing through the aforementioned tendinous sheaths.

After the aforementioned incisions were made and ROIs were exposed, the surgeon selected thirteen sites which according to anatomical references potentially contained nerve tissue. Particularly sites which could contain connective tissue and blood vessels in addition to nerve tissue were selected to compare the optical behavior of the tissues. The surgeon subsequently assessed whether the selected sites actually contained nerve and/or other tissues. The surgeon removed tissue from seven sites for independent *ex situ* assessment using the CPLi system. Subsequently, the surgeon appointed the remaining six sites to be observed *in situ* by CPLi. The CPLi operator, blinded to the assessments of the surgeon, independently recorded dichotomously whether the samples/sites contained nerve tissue or not, followed by histological verification by an independent pathologist.

Histological evaluation

Histological evaluation of the thirteen tissue samples was performed to confirm the presence or absence of nerve tissue at the department of Pathology using standard clinical histopathological methods. We considered this the gold standard. The results of the tissue samples obtained with *in situ* examination by eye or via the CPLi system were not disclosed to the pathologist in order to obtain non-biased results.

Preliminary in vivo observations

After the observations in cadaver tissue, preliminary observations were performed *in vivo* on one patient using CPLi during a surgical intervention at the carpometacarpal joint for chronic pain relief.

Results

Examination of the nerves of the unfrozen and thawed pig tissue, resulted in no alteration of the observed anisotropic optical reflection of the nerves after freezing (Appendix 1).

Tissue identification by the surgeon, CPLi and histopathology are presented in Table 1. Intraoperative identification of nerve tissue by the surgeon was accurate in ten of the thirteen samples (77%) as compared to histopathology. Intraoperative identification using CPLi was

Biomedical Optics EXPRESS

correct in 100% of the samples regarding the presence of nerve tissue, as confirmed by histopathological examination.

Table 1. Comparison of the presence of nerve tissue

Sample	Tissue type according to surgeon	Presence of nerves according to CPLi (yes/no)	Pathologist
1	Blood vessels	yes	Nerve tissue, blood vessels
2	Nerve tissue	yes	Nerve tissue, adipose tissue
3	Fascia, connective tissue	No	Adipose tissue, connective tissue
4	Tendon	No	Tendon
5	Blood vessel	No	Blood vessel
6	Possible nerve tissue	yes	Nerve tissue
7	Possible nerve tissue	yes	Nerve tissue
8	Nerve tissue	yes	Nerve tissue
9	Fascia	No	Connective tissue
10	Tendon	No	Tendon
11	Nerve tissue	yes	Nerve tissue
12	Blood vessel	No	Blood vessel
13	Nerve tissue, fascia	yes	Nerve tissue

CPLi: Collimated polarized light imaging

Macroscopical observations of human cadaver tissue

The images in Fig. 3 show the observations as assessed during the surgical intervention by eye and with the CPLi system. Figure 3(A) shows the superficial subcutaneous tissue under conventional surgical illumination after opening the skin at the dorsoradial part of a human hand (tabatière region). Figure 3(D) shows the deeper-lying subcutaneous tissue. Conventional illumination allowed only minimal visual distinction of the different tissue types; only the blood vessels (indicated by the red arrows) could be clearly distinguished by their color. Visualization using the CPLi system revealed tissues possessing a clear anisotropic optical signature as illustrated in Figs. 3(B), 3(C), 3(E) and 3(F). These tissue structures indicated by the black arrows show a distinct 'on and off' switching of the optical reflection with every 45° rotation of the polarization unit (red box, Fig. 1) with respect to the orientation of the tissue. This 'on and off' switching upon dynamic rotation of the polarization unit is a unique feature of nerve tissue, confirming the presence of a nerve at these sites surrounding the blood vessel [23]. The blue arrows in Figs. 3(B), 3(C), 3(E), 3(F) indicate tissue structures which remain unchanged in contrast to the nerve tissue. The yellow arrows shown in Figs. 3(C) and 3(F) point at nerves that have optically nearly disappeared compared to Figs. 3(B) and 3(E) upon rotation of the polarizer unit. The size range of the aforementioned nerves observed in Fig. 3 is less than 1 mm in width (the scale bar represents 5 mm).

Tissue identification of larger anisotropic tissue structures can sometimes be mistaken under normal visual identification as well. Therefore also the larger elongated structures (3 – 4 mm in width) were examined with the CPLi system. Figures 3(G) and 3(J) show tissue around the dorsal area of the wrist and forearm (articulatio radiocarpea). In Fig. 3(G) two elongated tissue structures are shown under conventional surgical illumination (yellow arrows), where both these elongated tissue structures have a white appearance. Further examination using the CPLi system (Fig. 3(H)) reveals a pearlescent appearance for the upper structure (blue arrow) while the lower structure (black arrow) exhibits a diffuse white appearance. Upon dynamic rotation of the CPLi system the upper structure maintains its pearlescent appearance while the lower structure reveals the nerve specific 'on and off' switching of the white reflection (Fig. 3(I)). Therefore, based on the anatomical location and the optical properties observed, the

Biomedical Optics EXPRESS

structure with a pearlescent appearance is identified as a tendon of the extensor carpi radialis longus muscle, whilst the lower structure is identified as part of the dorsal digital nerve of the radial nerve.

To assess the contrast in anisotropic optical effects between the different structures, multiple sites around the aforementioned tabatière region were observed during the surgical intervention; this also revealed areas with nearly no anisotropic optical effects. Figure 3(J) shows an example of the area around the deeper situated radial artery at the tabatière region using the CPLi system. No clear difference of the polarized reflection upon dynamic rotation of the CPLi system was observed here, indicating the absence of nerve tissue at this site (Figs. 3(K), 3(L)).

In the supplemental material, videos illustrating the real-time nerve specific 'on and off' switching of the nerves on the superficial subcutaneous tissue (Figs. 3(B), 3(C)), deeper lying tissue (Figs. 3(E), 3(F)), and nerves in comparison with the larger (tendinous) structures (Figs. 3(H), 3(I)) can be found. The first video (Visualization 1) clearly shows the appearing and disappearing of the white strands pointed out in Figs. 3(B) and 3(C) (black and yellow arrows). The second video (Visualization 2) show the appearance and disappearance of numerous small white strands, surrounding the red blood vessel and in the surrounding fatty tissue. Lastly the third video (Visualization 3) illustrates the difference in optical behavior of tendons versus the nerves. The tendon has a distinctly different pearlescent appearance which behaves differently from the 'on and off' switching of the adjacent nerve.

Biomedical Optics EXPRESS

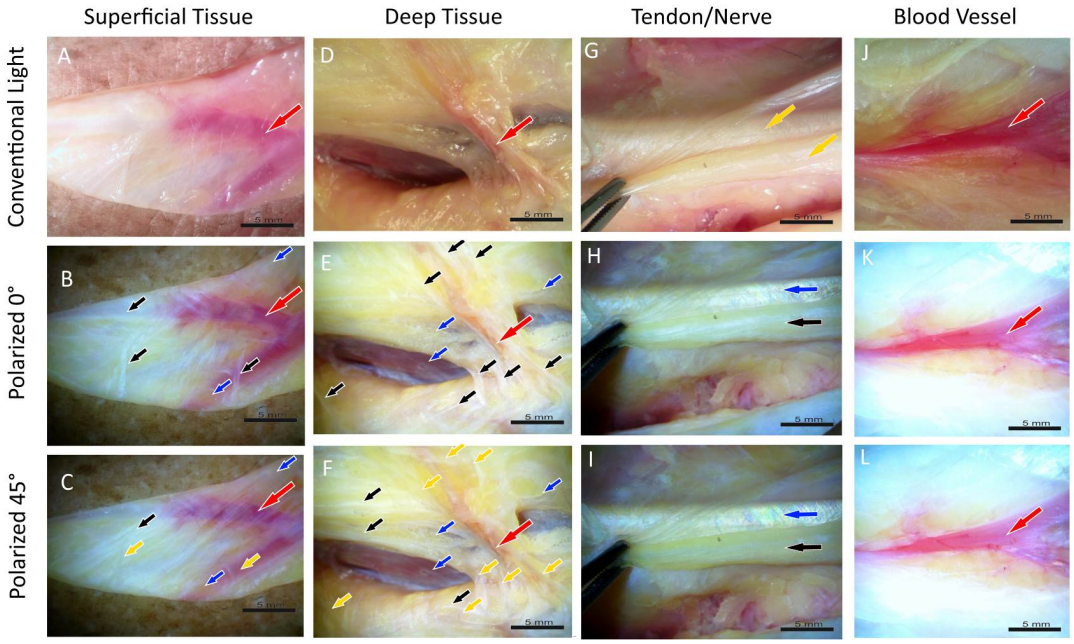

Fig. 3. A-F. The incision exposes the subcutaneous tissue at the dorsoradial part of a human hand near the tabatière region. (A,D): Using conventional surgical illumination, the blood vessel can be clearly distinguished from other (connective) tissue, at the exposed superficial and deep-lying subcutaneous tissue. (B,E): Observing the same ROI using CPLi (see Visualization 1 and Visualization 2), reveals a bright white reflection of the nerves (black arrows) which are less than 1 mm in width. (C,F): The cross polarizers are rotated 45° with respect to the position of the cross polarizers in figures B and E. This results in a reduction of the optical reflection of the nerve tissue depicted in B and E, representing the 'switched off state' (yellow arrows). In contrast other nerves are now visible in C and F (black arrows) because of their different orientation relative to the orientation of the polarizers in B and E. At the blue and red arrows no clear difference is observed which indicates the absence of nerve tissue. Figure 3G. The two elongated structures are shown at the articulatio radiocarpea on the dorsoradial hand. Under conventional illumination, the two elongated tissue structures designated with the yellow arrows possess a nearly identical optical appearance. (H): Using CPLi (see Visualization 3) the upper elongated (blue arrow) structure reveals a pearlescent appearance and can be identified as the tendon of the extensor carpi radialis longus whilst the lower elongated structure (black arrow) shows an oriented white reflection which indicates a branch of the digital dorsal nerve of the radial nerve. (I): Compared to panel H the characteristic 'on and off' switching of the polarized reflection of the nerve tissue is apparent upon rotation of the polarizer unit, as the white reflection in panel I is reduced. The tendon however, retains the same pearlescent appearance. Figure 3J. The red arrow in both pictures marks the radial artery located between the thumb and the index finger. The radial artery at the red arrow in panel K shows no clear difference in optical reflection upon dynamic rotation of the polarization unit compared to panel L.

Preliminary in vivo observation in human tissue

Based upon the observations in cadaver tissue, the use of CPLi was explored *in vivo*. With consent of the patient, the area around the carpometacarpal joint was observed for presence of nerve tissue during a surgical intervention for relief of chronic pain. It was confirmed during this operation that the anisotropic optical signature of nerves was also visible *in vivo*. This is shown in Fig. 4 in which the nerve specific 'on and off' switching was observed at a region with various different tissue structures which were in close proximity of each other, difficult to identify by eye. Upon dynamic rotation of the polarization unit of the CPLi system (Fig. 1) the vertical structure indicated by the blue arrow appears brighter in Fig. 4(B) versus the same

Biomedical Optics EXPRESS

in Fig. 4(A), whilst the opposite is observed for the oblique structure pointed by the green arrows, indicating the presence of nerve tissue.

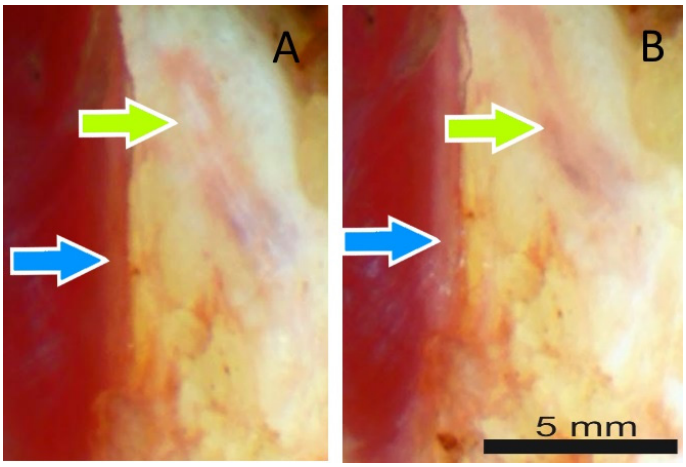

Fig. 4. The blue arrow highlights a vertical structure (A), which appears whiter after rotating the polarizers (B). The opposite occurs at the oblique structure (green arrow) indicating nerve tissue.

Discussion

One of the main reasons of accidental nerve injuries during a surgical intervention is the difficulty of visual identification of the different tissue types encountered [2]. Fresh frozen human tissue was suitable for this experiment, due to the fact that freezing had no adverse effect on the anisotropic optical reflection of the nerve tissue of the thawed pig tissue. The results of the first CPLi observations in human (cadaver) tissue have shown that it is possible to identify human nerves in real-time and with greater reliability than by normal visual identification by the surgeon. In contrast to for example OCT, CPLi does not need any image processing afterwards to create an image of the ROI and can also image a much larger area at one time. The long working distance of our CPLi system avoids physical/mechanical contact with the nerves during identification as opposed to ultrasound or IONM. This prevents unnecessary damage to nerves due to traction on the nerves during identification [10]. In addition, the long working distance between the CPLi system and the patient makes the system suitable for surgical interventions in deeper structures, such as the tendinous sheath of the wrist which is opened in case of *de Quervain* tendinopathy [10]. In this area it is particularly challenging to visually distinguish the nerves from other surrounding tissue types under conventional surgical illumination. A clear example in our cadaver experiment where nerves could be spared is in the subcutaneous tissue, where nerve tissue is easily mistaken for connective tissue by eye under conventional surgical illumination. This is a type of structure which, according to the surgeon, is often inadvertently cauterized. These small 'hidden' nerves are typically prone to accidental nerve damage during surgical interventions as they cannot be identified by eye under conventional surgical illumination. Therefore our CPLi system is suitable in preventing unnecessary nerve damage in a wide variety of surgical interventions in which nerve preservation is vital.

Future improvements will focus on increasing the field of view of CPLi, even though it is already larger than that of OCT (square centimeters vs square millimeters), to further expand its clinical applicability. The preliminary results of observations using CPLi in a live patient seem promising. Additional *in vivo* CPLi observations in a larger patient cohort will be conducted to compare the optical behavior of nerve tissue between patients and during varying surgical conditions.

Biomedical Optics EXPRESS

Conclusion

The results of CPLi on human cadaver tissue at the dorsoradial side of a human hand have shown the feasibility of using the unique anisotropic optical properties of nerve tissue for real-time non-invasive identification. CPLi proved to be a fast and reliable technique when comparing CPLi with conventional inspection under customary surgical illumination. Using CPLi, it was possible to identify nerves in real-time with a 100% positive score rate. The *in vivo* observations during an actual operation using the CPLi system confirm the *ex vivo* observations. The CPLi system has shown clear potential to improve the identification of nerves during a surgical intervention.

Appendix 1: optical behavior of nerve tissue after freezing and thawing

For this study the effect of freezing on the optical behavior of nerve tissue had to be determined, due to the fact that the human tissue necessary for the experiment was not chemically conserved. Instead the tissue was preserved by freezing. Therefore the possible consequences freezing have on the anisotropic optical properties of nerves had to be determined.

It is known that freezing and thawing tissue has negative implications for the cellular structure. The rate at which the nerve tissue is frozen, also determines where the formation of ice crystals occurs. In most soft tissue cells, slow freezing does not cause gross membrane rupture [25].

The study by Zhu et al. further confirmed that that slowly freezing and fast thawing produces the least amount of damage to the nerve tissue, such as demyelination, axon exposure or discontinuity [26].

The temperature at which the nerve tissue is stored influences the amount of cellular damage. The least amount of changes occur between −5 and −10°C, however below −15°C results in ruptures in the myelin and separation of the lamellae [27-28].

To study the effect of freezing a substitute for human tissue in the form of pig tissue (Sus scrofa) has been used. Pig tissue that has never been frozen, has been used as our control. A site was selected that revealed the characteristic nerve specific anisotropic optical reflection, i.e. the ‘on and off’ switching of nerve tissue using CPLi. Images of this site were made (Fig. 5) prior to freezing. The site was then marked and assessed again after the tissue had been frozen and thawed (Fig. 6).

Biomedical Optics EXPRESS

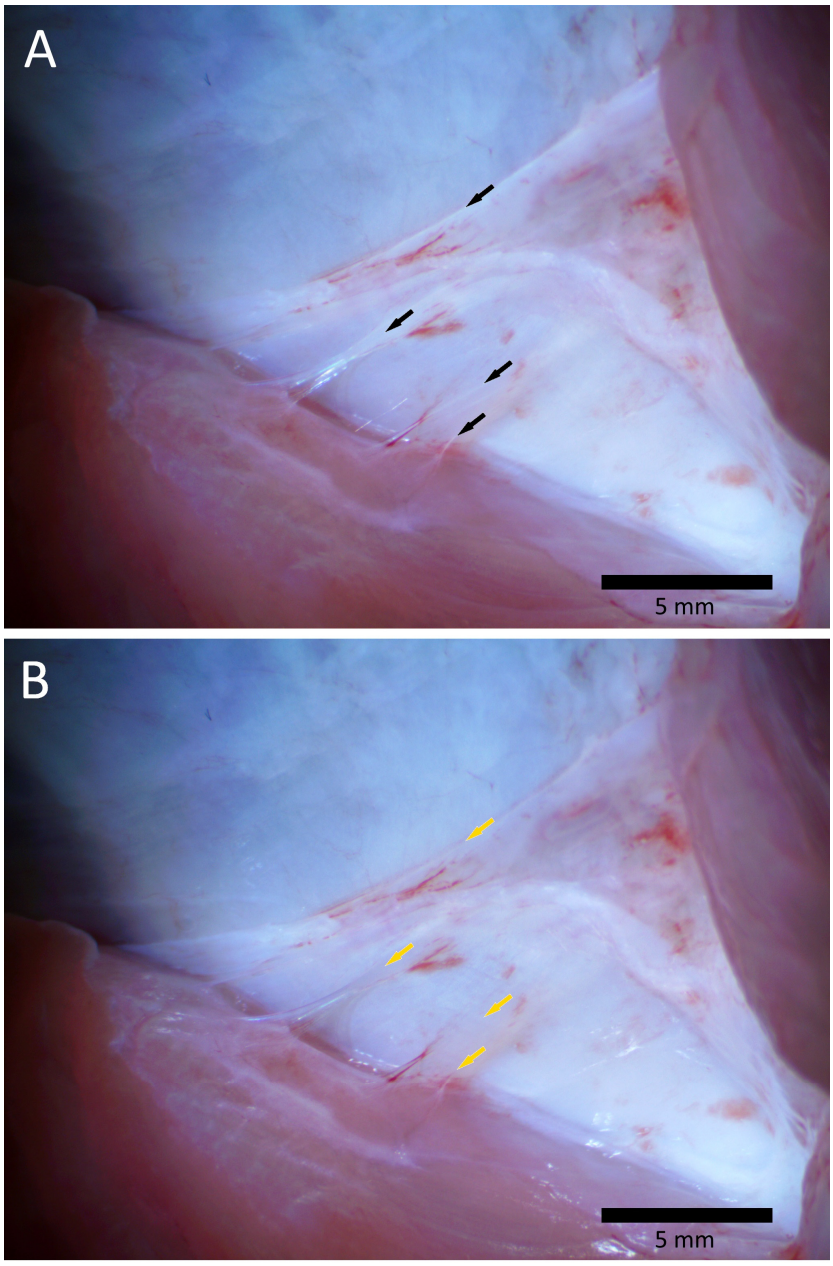

Fig. 5. (A) Prior to freezing, the structures marked with the black arrows appear white indicating that the nerves are oriented 45° to the cross polarizers. (B) The same areas marked with the yellow arrows now appear to be translucent, when aligned with either one of the cross polarizers.

Biomedical Optics EXPRESS

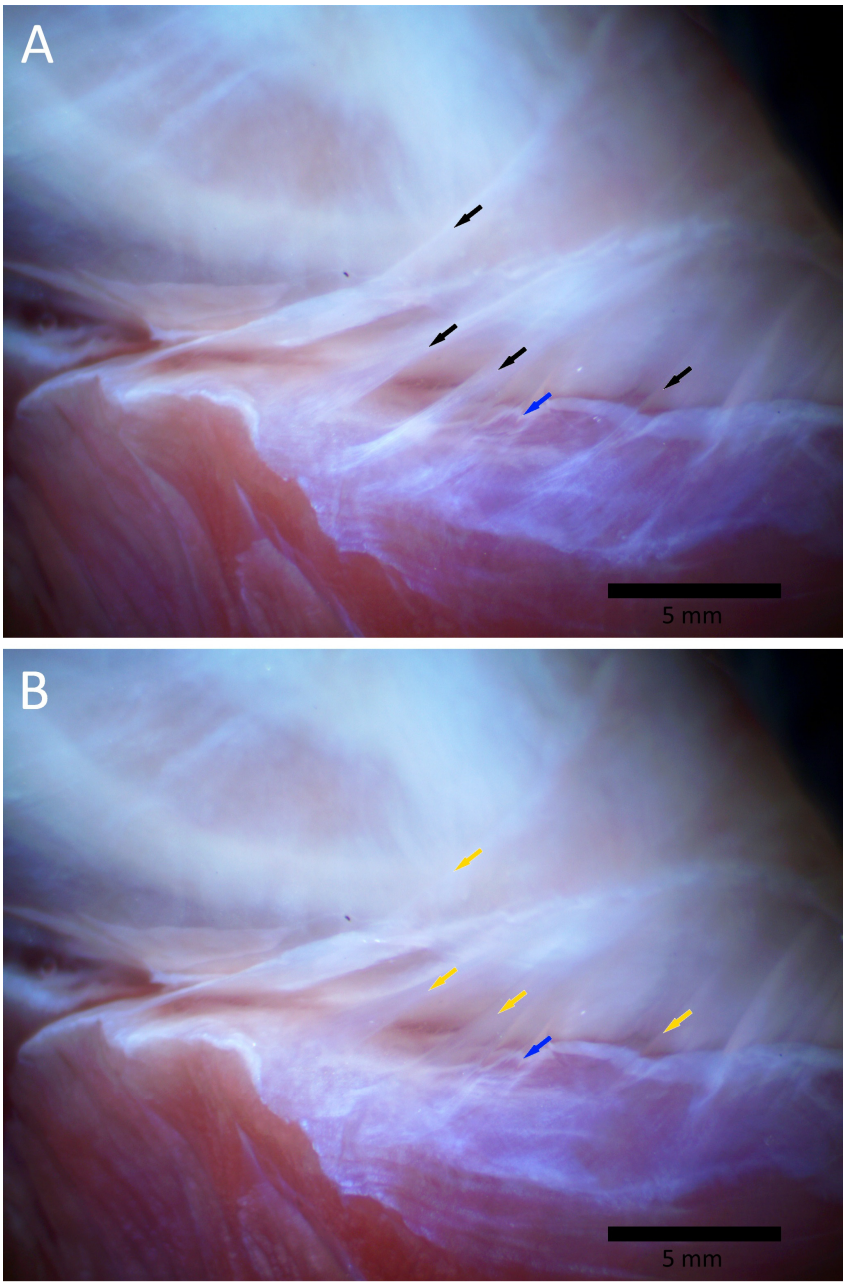

Fig. 6. (A) The same region of interest after freezing and thawing, the structures marked with the black arrows appear to be bright white indicating that the nerves are oriented 45° to the cross polarizers. (B) The same areas marked with the yellow arrows now appear translucent, when aligned with either one of the cross polarizers. The tissue at the blue arrows in both images remains unchanged, indicating that it does not consist out of nerve tissue.

Images prior and after freezing and thawing show similar results on a macroscopic level using CPLi.

Validation of the observed tissue was performed using conventional polarization microscopy (PLM). Figure 7 shows the tissue under the polarization microscope. The anisotropic properties of the nerve tissue are clearly observable. When the nerve is parallel to

Biomedical Optics EXPRESS

one of the cross polarizers, the polarized reflection is not observable. When rotated to 45°, a clear polarized reflection is observable. This clearly distinguishes the nerve tissue from the surrounding connective tissue.

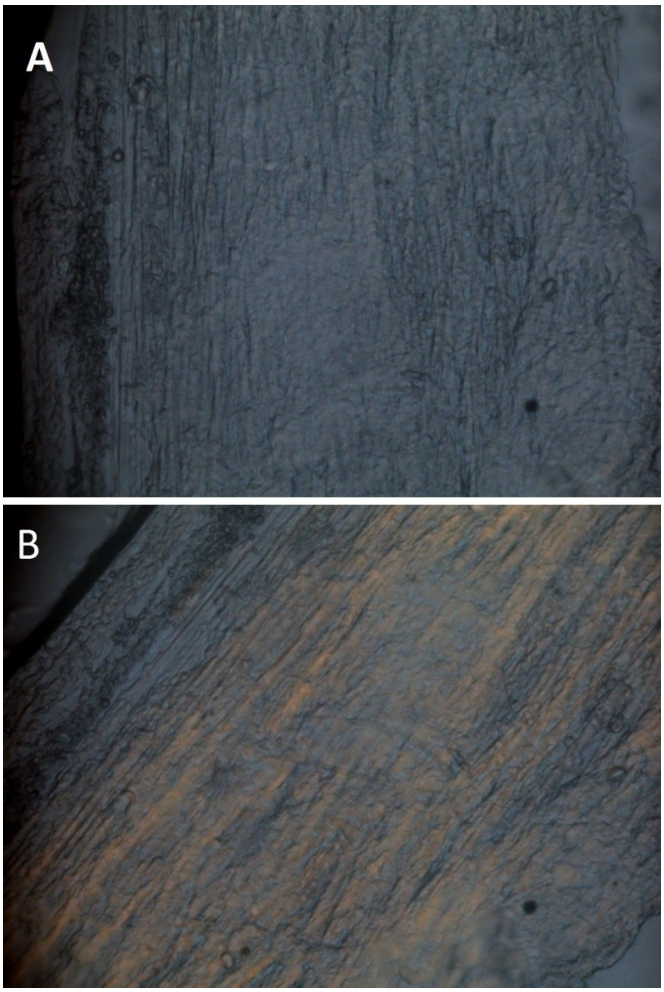

Fig. 7. (A) A sample identified as a nerve under conventional polarized light microscopy. The nerve is parallel to one of the cross polarizers, therefore the polarized reflection is not visible. (B) The nerve is rotated 45° to the polarizers, revealing an orange appearance, i.e. the nerve specific anisotropic optical reflection.

The results of the PLM confirm the presence of nerve tissue on a microscopic level, confirming the macroscopic observations. Therefore it was justified to use fresh frozen human tissue, due to the fact that freezing and thawing does not affect the characteristic nerve specific anisotropic optical reflection.

Acknowledgments

We would like to thank Ms. Julia H.E. Houtzager for the illustration of the tabatière region and Mrs. Esther E.M. Posno – Peltenburg for taking care of the tissue processing and logistics.

Disclosures

The authors declare that there are no conflicts of interest related to this article.